SPINE Volume 18, Number 16, pp 2457–2464

Three-Dimensional Simulation of Harrington Distraction Instrumentation for Surgical Correction of Scoliosis

I. A. F. Stokes, PhD, and M. Gardner-Morse, MSME

Harrington distraction rod surgery on six female patients with idiopathic scoliosis was simulated in three-dimensional osseoligamentous finite element models with individual geometry taken from preoperative stereo roentgenographic reconstructions of the spine and ribcage and compared with the measured outcome. Boundary conditions at the ends of the spine were used to maintain pelvis and head alignment. Published material and flexibility properties were used. The amount of hook distraction was calculated from measured changes in the distance between the hook sites (range, 13–27 mm). Initial simulations underestimated the Cobb angle correction by an average 6%. They underestimated the spinal elongation by 36% and predicted an average 12° increase in kyphosis angle compared with an actual 10° average decrease. Agreement for sagittal plane changes improved in five cases when the beams representing the motion segments were displaced posteriorly. In the sixth case (with the rod applied over a lordotic spinal region), agreement was improved with the motion segment beams displaced anteriorly. The amount of the beam displacement that gave the best agreement was variable, and we were not able to predict it for each individual. Both measured and simulated changes in vertebral transverse plane rotations and in rib angulations were small. The greatest source of errors in these simulations appeared to be inadequate representation of in vivo motion segment behavior by in vitro measured stiffness properties. [Key words: spine, scoliosis, biomechanics, surgery, Harrington instrumentation, finite elements]

A surgeon planning individualized surgical treatment of spinal deformity must decide which instrumentation to use and the vertebrae to which it will be applied, but the relationship between these variables and the final outcome is not well defined. The information that can be used in this decision-making process consists of clinical studies, laboratory testing of implants, animal testing, and preoperative studies of an individual patient. This report is concerned with the possibility of using preoperative simulations of the surgery to augment this process. Such a model could be used to simulate variations of surgery such as the selection of hook levels, and predict the three-dimensional outcome in terms of deformity correction and flexibility of the construct.

Existing sources of information provide incomplete information for preoperative planning. Clinical studies with large groups of patients compare the relative value of competing surgical procedures. Although the effect of Harrington instrumentation on the frontal plane shape of the spine has been well described,[4,5,8,9,18,20,36] its effect on the three-dimensional shape of the spine and ribcage and the mechanism of action are poorly understood. Clinical studies in humans undergoing surgery can be inconclusive, especially because of variation in spinal shape and flexibility, and difficulties in documenting postoperative changes. Mechanical testing of spinal instrumentation in the laboratory relies on animal spines[3,16,21] or undeformed cadaver spines[22] with questionable relevance to in vivo use. These tests also need large statistical samples of animals or spinal specimens to deal with biologic variability. Live animal studies are required to assess the long-term results after implantation of instrumentation.

These problems expose the need for analytic methods to explain the relationships between surgical choices, individual variations, and the outcome of surgery. Of several previous attempts to develop biomechanical models of scoliosis surgery,[12,14,19,24,26,27,34,37] only Schultz and Hirsch[26,27] investigated differing preoperative spinal shapes in three-dimensional models, but these models did not include the individual sagittal plane spinal shape nor the individual amount of hook distraction, and they omitted the rib cage.

This article reports on finite element simulations of Harrington rod distraction surgery used to correct idiopathic scoliosis in six patients. These models used individualized geometry from three-dimensional stereo roentgenographic measurements[7,31] of each patient. The predicted changes were compared with stereo roentgenographic measurements that documented the postoperative changes. The objectives of this work are to develop and validate a model of the biomechanical behavior of the spine and ribcage that could be used before surgery

From the Department of Orthopaedics and Rehabilitation, University of Vermont, Burlington, Vermont.
Supported by NIH R01 AR 40093.
Accepted for publication December 29, 1992.

Table 1. Preoperative Patient Details

			Thoracic Curve			Lumbar Curve		
Patient No.	Age at Surgery (Years)	King Type*	Cobb Angle (Degrees)	Upper-Apex-Lower Levels	Apex Axial Rotation (Degrees)	Cobb Angle (Degrees)	Upper-Apex-Lower Levels	Apex Axial Rotation (Degrees)
1	13.4	III	44	T7-T11-L2	20	—	—	—
2	12.9	I	50	T6-T8-T11	8	58	T11-L2-L5	19
3	15.7	II	33	T6-T8-T12	2	45	T12-L2-L5	5
4	14.8	II	45	T5-T8-T11	14	35	T11-L3-L5	2
5	14.3	III	43	T7-T10-L1	13	—	—	—
6	12.5	II	54	T6-T9-T12	12	37	T12-L2-L4	4
Mean	13.9	—	45	—	12	44	—	8

From reference 18.

to predict the effects of spinal surgery on scoliosis deformity, taking into account different instrumentations and differences between individuals. The purpose of this report is to test the application of this model to simulation of Harrington distraction rod surgery. We chose to study this instrumentation first because of its relative simplicity compared with the newer, more complex designs of instrumentation.

■ Methods

Six female adolescent patients with idiopathic scoliosis who had spinal arthrodesis with Harrington rods were studied (Table 1). The three-dimensional shape of each patient's spine and ribcage was measured by stereo radiography[7,31] before and after surgery. The measured preoperative shape was used to define the geometry of the finite element model for each patient. The models consisted of the osseoligamentous components of the thorax and spine (Figure 1). The model, and its validation against published flexibility measurements, was reported by Stokes and Laible.[32] The motion segments were represented by beam elements[11] matched to experimentally derived stiffness matrix data.[23]

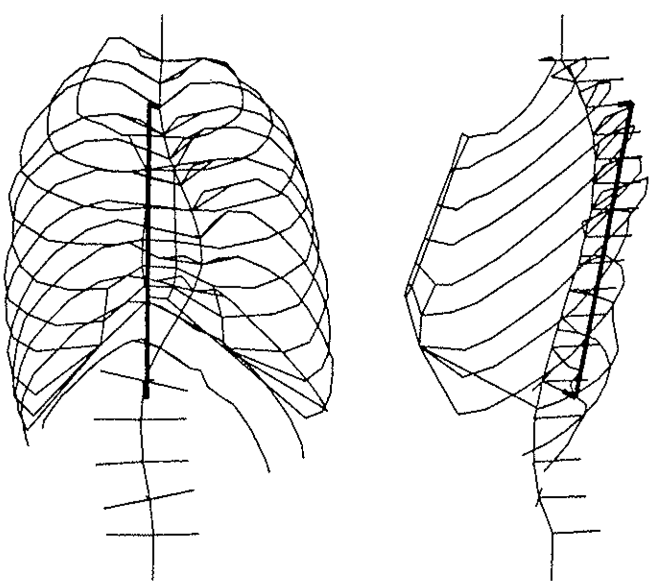

Figure 1. Preoperative posteroanterior and lateral view (right side) of model of Patient 6. The geometry was obtained from three-dimensional stereo roentgenographic measurements[7] of this patient. Each straight line represents a beam finite element. Thin lines represent the ribs, motion segments, and sternum, and thick lines represent the Harrington rod and hooks. Intercostal ligaments and the left hemithorax in the lateral view were omitted for clarity.

The Harrington rod was represented by up to three straight beam elements, depending on its curvature. The rod had a diameter of 7 mm, with material properties corresponding to stainless steel. The hook-to-vertebra connections allowed rotation around the local x and y axes of the hook (Figure 2), but not around the z axis, for model stability. The upper hook was free to rotate around the Harrington rod, and the lower hook was attached rigidly to the rod, also for reasons of stability.

"Righting forces"[13,25] maintain the alignment of the head above the pelvis, without axial rotation. To simulate these reflex muscle contractions, model boundary conditions were used to constrain motion at the end vertebrae (C7 and the sacrum). The sacrum could only rotate in flexion–extension and C7 could only translate vertically and rotate in flexion–extension.

To simulate the surgery, a displacement was applied to hooks connected to the vertebrae selected for the actual surgery. The relative displacement of the hooks was calculated from the preoperative and postoperative stereo roentgenographic reconstructions. The amount of hook distraction was the difference between the predistraction and the postdis-

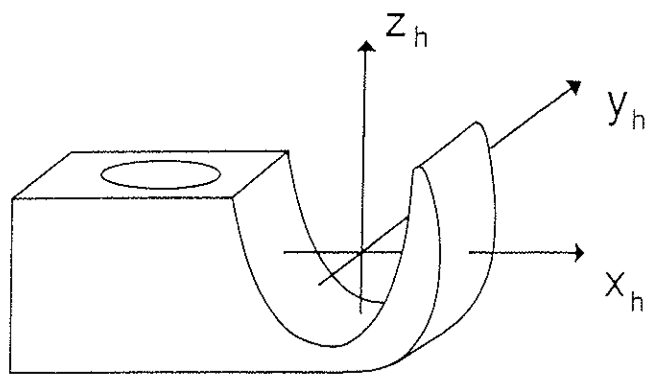

Figure 2. Local axis system for hooks.

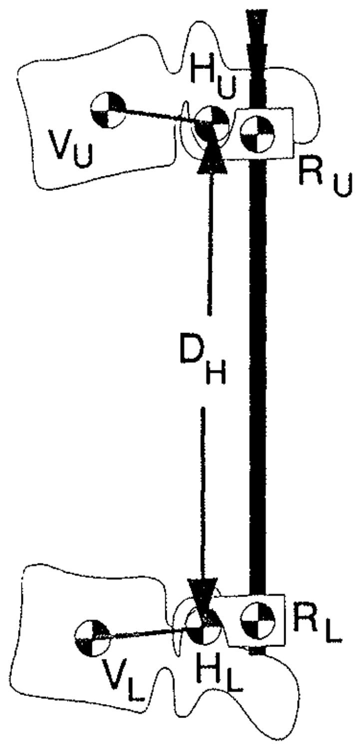

Figure 3. Geometry used to calculate hook distraction during surgery. The problem was to measure the distance D_H both before and after surgery. Points V_U and V_L were measured both before and after surgery, together with the angulation of the corresponding vertebrae. Points R_U and R_L were measured after surgery. These measurements allowed calculation of the position of points H_U and H_L.

traction positions of the hooks. The postdistraction positions were measured from the postoperative radiographs (Figure 3).

The preoperative positions of the points H_U and H_L (Figure 3) were calculated from the measured preoperative positions of the vertebral centers, together with measurements of the changes in the frontal and sagittal plane vertebral angulations (Figure 4). Changes in the transverse plane angulations (axial rotations) of these vertebrae were small and were ignored. The calculated hook distraction had a mean of 20.4 mm (range, 13–27 mm, Table 2).

The input to the finite element model was the calculated hook distraction represented as a thermal expansion of the rod. A finite element program (HyperSap, Algor Interactive Systems Inc., Pittsburgh, PA 15238) was used to calculate the resulting changes in model geometry and the forces generated in the rod, using a single linear stiffness calculation. The linear model appeared justified because only small geometric differences (less than 2° Cobb) were found when a large displacement (geometric nonlinearity) analysis was compared with the linear model. The greatest difference was that the nonlinear analysis predicted larger Harrington rod forces.

Spinal curvatures and rotation and asymmetry of the ribcage were calculated by a method described previously.[7,31] The following measures were used to quantify preoperative, postoperative, and simulated postoperative shape of each patient:

1. Spinal elongation. This was defined as the increase in the three-dimensional linear distance D_V (Figure 5) between the centers of the vertebrae at the hook levels.

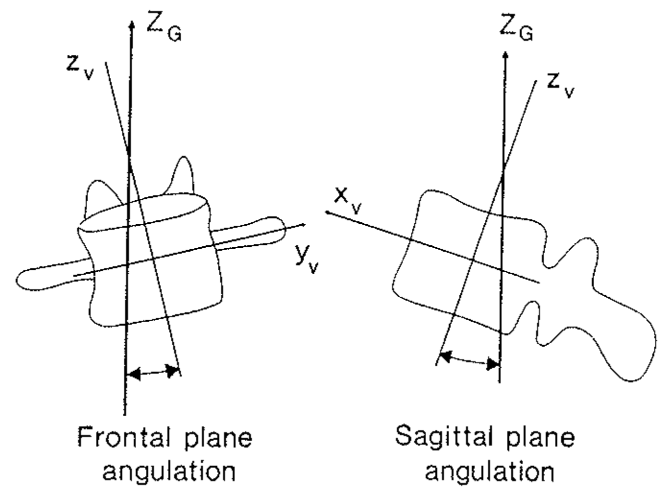

Figure 4. Definitions of vertebra angulation measurements. Sagittal and frontal plane angulations of vertebrae are defined as the angles between local (x_v, y_v, x_v) and global (X_G, Y_G, Z_G) axes, when projected on to the global sagittal and frontal planes.

2. Changes in the relative frontal and sagittal plane angulations of the vertebrae at hook levels (Figure 5).
3. Scoliosis analytic Cobb angle (hereafter Cobb angle). This was defined as the angle between normals at inflection points on the frontal plane projection of the line passing through vertebral body centers.[31]
4. Kyphosis angle and lordosis angle measured as the angles between normals at inflection points on the sagittal plane projection of the line passing through vertebral body centers.
5. Apical/vertebral axial rotation, using the method of Stokes et al.[29,30] These measurements were averaged from available preoperative and postoperative films.
6. Posterior rib rotation was measured as the angulation to the frontal plane of the double tangent line between the posterior margins of the right and left ribs of the same anatomic level.[7,28]
7. Frontal plane rib angle was measured as the angle, as viewed from the front, between a plane fitted though the rib and a transverse plane. Lateral plane rib angle was measured as the angle, as viewed from the side, between a plane fitted though the rib and a transverse plane.[7]

Simulations were made using a baseline model, and

Table 2. Harrington Hook Levels, Measured Rod Distraction, and Baseline Model Calculated Rod Distraction Force

Patient No.	Upper-Lower Hook Levels	Rod Distraction (mm)	Rod Distraction Force (N)
1	T4-L2	16	306
2	T5-L4	26	573
3	T5-L4*	27	199
4	T3-L1*	18	529
5	T3-L1*	22	693
6	T3-L1	13	362
Mean (SD)		20.4 (5.7)	444 (185)

*Contoured (curved) Harrington rod.

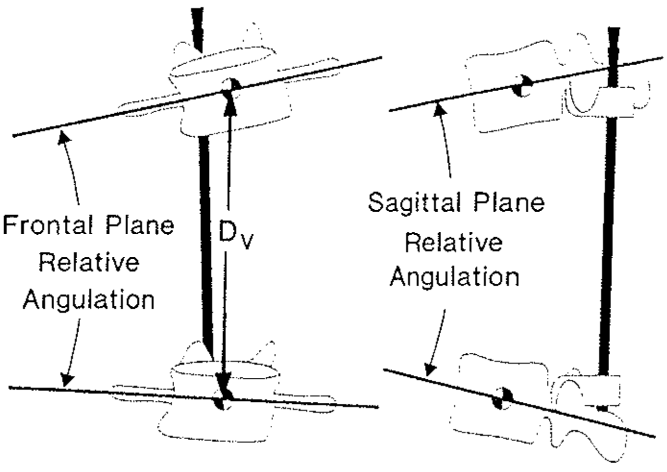

Figure 5. Definition of frontal and sagittal plane relative angulation and distance between vertebrae D_V. Spinal elongation was defined as change in the distance D_V. These measurements were used to characterize the measured and simulated changes in spinal shape between vertebrae to which distraction instrumentation was attached.

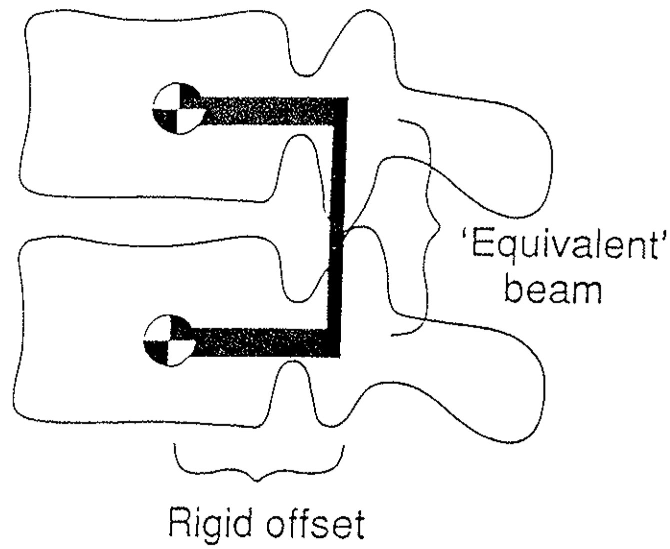

Figure 6. Model representation of the motion segment by an "equivalent" beam with a variable rigid offset.

variations from it, to investigate the sensitivity to motion segment properties, boundary conditions, and ribcage flexibility. Preliminary studies[33] using this model showed worse agreement with postoperative measurements in the sagittal plane than in the frontal plane, suggesting that the motion segment beams were incorrectly representing the in vivo behavior of the spine. In the models R10, R-10, R-20, and R-30, rigid offsets in the anterior (positive) or posterior (negative) direction were applied to motion segment beams to translate them (Figure 6). These rigid offsets altered the relationship between the motion segment sagittal plane rotation and translation motion in response to forces in the sagittal plane. The amount of the rigid offset was 10, −10, −20, or −30 mm. The effect of such rigid translations on the beam stiffness matrix is given by Weaver and Gere.[39]

Sensitivity to model boundary conditions was investigated by removing the end constraints in lateral bending at C7 and the sacrum and axial rotation at C7. This resulted in a minimally constrained model without any forces transmitted through the end constraints. To study sensitivity to the rib cage, the intercostal connections were first removed, then the ribs themselves were removed from the models.

■ Results

Baseline Model Results

The frontal plane correction (Cobb angle) was slightly underestimated by the model compared with that measured after surgery (Table 3). In the sagittal plane, the simulations predicted curvature changes in the opposite direction in most cases compared with the measured changes (Table 4). The simulations predicted no change on average in the relative angulations of the vertebrae at hook levels, whereas the measured values decreased by an average of 11°. The difference between simulations and postoperative measurements were more pronounced at the upper hook than at the lower hook level. The spinal elongation in the baseline simulations (mean, 13.1 mm) was less than that measured (mean, 20.5 mm) in all six patients (Table 5). Thus, overall the agreement was better in the frontal plane than the sagittal plane, where the models predicted an incorrect relationship between spinal elongation and relative angulation of hooked vertebrae.

Table 3. Measured and Baseline Model Simulated Changes in Frontal Plane Cobb Angles and Relative Angulation

	Thoracic Curve Cobb Angle Change				Lumbar Curve Cobb Angle Change				Relative Angulation Change (Hook Levels)			
	Measured		Simulated		Measured		Simulated		Measured		Simulated	
Patient No.	Degrees	%	Degrees	%	Degrees	%	Degrees	%	Degrees	%	Degrees	%
1	15	34	10	23	—		—		11	35	12	39
2	7	14	15	30	12	21	18	31	10	100	5	50
3	13	39	4	12	14	31	8	18	1	10	3	30
4	19	42	17	38	14	40	6	17	8	30	13	48
5	22	51	20	47	—	—	—	—	19	63	18	60
6	19	35	17	31	7	19	6	16	11	52	11	52
Mean	16	36	14	30	12	28	10	20	10	48	10	46

Table 4. Preoperative Conditions, Measured Changes, and Simulated Changes in Sagittal Plane Curvatures

	Kyphosis Angle				Lordosis Angle				Relative Angulation		
Patient No.	Upper-Apex-Lower Levels*	Preoperative (Degrees)	Measured Change (Degrees)	Simulated Change (Degrees)	Upper-Apex-Lower Levels*	Preoperative (Degrees)	Measured Change (Degrees)	Simulated Change (Degrees)	Preoperative (Degrees)	Measured Change (Degrees)	Simulated Change (Degrees)
1	T2-T9-L1	20	−6	13	L1-L4-L5	18	−11	−3	17	−10	10
2	T10-L1-L5	31	5	25	—	—	—	—	30	−3	0
3	T1-T4-T10	20	−7	7	T10-L2-L5	57	−20	−17	34†	−24	−28
4	T8-T12-L3	35	−9	4	L3-L5-L5	33	−16	−6	14	−7	7
5	T1-T6-L1	29	−9	17	L1-L3-L5	77	−18	0	24	−11	7
6	T1-T6-T11	51	−33	5	T11-L3-L5	45	−17	0	32	−13	4
Mean	—	31	−10	12	—	46	−16	−5	25	−11	0

*Preoperative kyphosis and lordosis levels. Postoperative apex levels shifted as much as four levels from the preoperative levels.
†This patient had a lordotic relative angulation between hook levels. All other patients had kyphotic relative angulation between the hook levels.

Table 5. Measured and Simulated Spinal Distraction

		Simulations*					
Patient No.	Measured (mm)	R10 (mm)	Baseline (mm)	R-10 (mm)	R-20 (mm)	R-30 (mm)	MR (mm)
1	19.7	—	8.5	10.2	14.7	19.3*	8.8
2	26.4	—	21.7	27.1*	31.7	33.5	20.6
3	14.9	14.5*	12.5	10.4	9.1	11.5	12.9
4	18.9	—	12.3	15.2	18.7*	20.7	12.4
5	23.0	—	13.7	17.6	23.0*	25.9	13.1
6	20.2	—	10.1	12.4	14.8	16.2*	10.1

Measured and Simulated Changes in Sagittal Plane Relative Angulation

		Simulations*					
Patient No.	Measured (Degrees)	R10 (Degrees)	Baseline (Degrees)	R-10 (Degrees)	R-20 (Degrees)	R-30 (Degrees)	MR (Degrees)
1	−10	—	10	4	−6	−15	9
2	−3	—	0*	−18	−29	−31	2
3	−24	−25*	−28	−33	−35	−31	−28
4	−7	—	7	−4 *	−13	−17	7
5	−11	—	7	−6 *	−19	−23	6
6	−13	—	4	−3	−10	−13*	4

R10 = rigid offset of 10 mm (anterior) in equivalent beams. R-10 = rigid offset of −10 mm (posterior) in equivalent beams. R-20 = rigid offset of −20 mm (posterior) in equivalent beams. R-30 = rigid offset of −30 mm (posterior) in equivalent beams. MR = model end constraints released. See text for model details. *Indicates the model having the best agreement with the measured values. A tie is indicated by an asterisk between the two models.

Patient 2 was an exception to these trends. She had a loss of correction of Cobb angle after surgery in that nonstereo roentgenograms taken 5 days after surgery showed correction close to that in the simulation, but subsequent stereo films showed that 56% and 60% of the correction of the upper and lower curves, respectively, had been lost. This implies that the hooks moved relative to the vertebrae, thereby contradicting the assumptions we used in calculating hook distraction. There also was a 5° measured increase in kyphosis angle in this patient, opposite to the change in the other five patients.

Patient 3 was the only patient whose Harrington rod spanned a lordotic part of the spine. She was also the only patient in whom the measured change in this angle was in the same sense as the simulated change in the baseline model.

Changes in vertebra rotation were small (the maximum change was a reduction of 9°) in both measurements and simulations. A similar trend was found for the posterior rib cage rotation. These rotations and changes in them were comparable to measurement precision (±7°). Changes in the rib angles were also small. Figure 7a shows there was on average a small increase in the downward angulation of the ribs as viewed from the front, and Figure 7b shows a similar trend for the baseline simulations, especially on the patients' left (convex side of the scoliosis). In the lateral views, the mean downward angulation of the ribs also

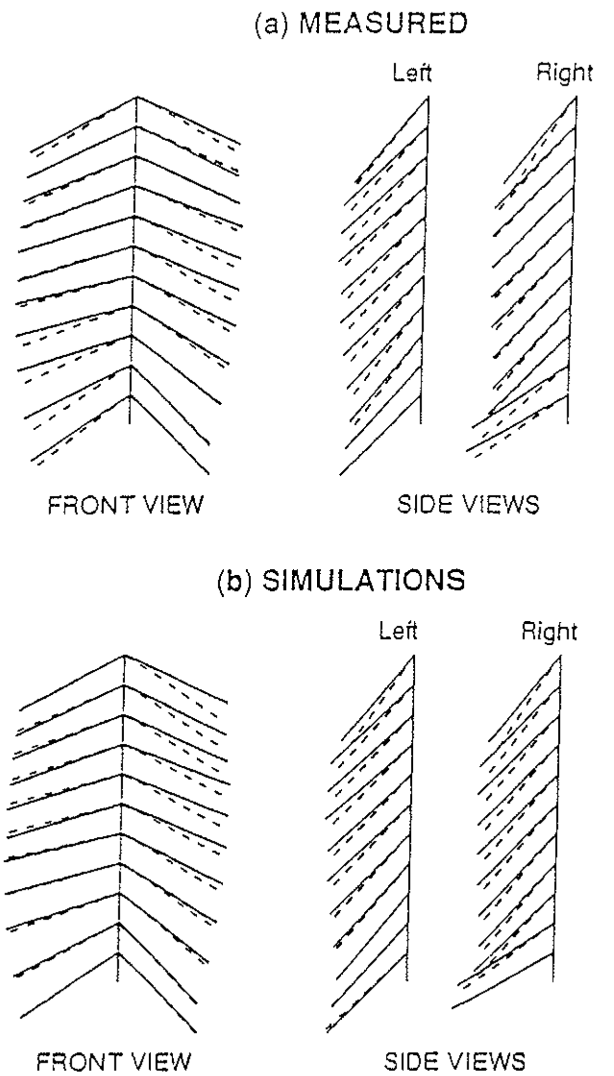

Figure 7. Representation of the frontal and lateral plane rib angles (mean for six patients) for rib pairs T1–T11 (T12 omitted from mean because one patient had only 11 rib pairs) (**a**) before and after surgery and (**b**) before surgery and according to the baseline simulations. The angle of each line relative to the horizontal in these diagrams corresponds to the mean of the measurements of the rib angles. Left: Frontal plane rib angles, as seen from the front. Center: Lateral plane rib angles (left side ribs). Right: Lateral plane rib angles (right side ribs). (**a**) Dash line = postoperative values; solid line = preoperative values. (**b**) Dash line = simulations; solid line = preoperative values.

increased slightly according to both the measurements and the baseline simulations.

Effects of Sagittal Plane Beam Offsets

The relationship between spinal elongation and change in angulation in the sagittal plane was expected to depend on the distance from the Harrington rod to the effective centers of the motion segments, because this would alter the ratio between the distraction force and the moments applied to the spine. In the R models (R10, R-10, R-20, and R-30) the motion segment beams had their longitudinal axes displaced a variable distance in the sagittal direction to alter this ratio. The rigid offsets gave improved agreement with measured results of surgery. Offsets in the range 0–30 mm of posterior displacement produced the best agreement with measured values of spinal elongation and sagittal plane angulation for five of the six patients (Table 5). In the case of Patient 3, the best results were obtained with the rigid offset in an anterior direction. This patient was different from the other five in that the Harrington rod spanned a lordotic region of the spine. Because an anterior offset gave the best results for Patient 3, the relationship between the amount of posterior displacement and the initial sagittal plane curvature was examined, but no correlation was evident. Thus, the amount of the motion segment beam rigid offset that gave the best agreement with measured values was not consistent, and we were not able to predict it accurately. The rigid offsets that gave the best agreement in the sagittal plane produced only small differences in the frontal plane (up to 2° less correction of the Cobb angle), but did change the rod forces (Table 6).

Sensitivity to Boundary Conditions

With the end of the spine unconstrained, there were lowered forces in the rods (Table 6), and very similar geometric changes in the instrumented region of the spine (Table 5). Correction of curves beyond the range of the instrumentation was slightly underestimated relative to the baseline models.

Sensitivity to Rib Cage

The main effect of removal of the rib cage was a 22% average reduction in the force associated with hook distraction. Most of this change occurred with removal of the intercostal elements, with little further change after removal of the ribs altogether. The greatest change in the frontal and sagittal plane relative angulations was 4°. In some patients there was minimal effect on the Cobb angle, but one patient showed 9° greater correction after removal of the rib cage. Changes in the transverse plane were less than 1°.

■ Discussion

As has been found in previous reports,[26,27] the agreement between the simulated and measured effects of surgery was good in the frontal plane. Our model also examined the sagittal plane, however, and showed that the response was very dependent on individual geometry and the

Table 6. Distraction Forces in Harrington Rods Expressed as Percentage of Baseline Models

	Patient No.					
Model	1	2	3	4	5	6
R10			71			
R-10	138	108	149	116	122	117
R-20	159	90	231	106	110	109
R-30	141	65	354	82	82	87
MR	77	86	92	82	79	84

representation of the motion segments. In this model, the individualized geometry of the spine, rib cage, and instrumentation explains some of the considerable variability in the results for different patients. This emphasizes the benefits of using three-dimensional individualized geometry in models to predict the outcome of surgery.

Agreement between the baseline simulation and measured changes in the sagittal plane was improved by adding rigid offsets to the motion segment beams, thus altering the ratio between moments and distraction forces applied to the instrumented part of the spine. This finding suggests that the published[23] flexibility behavior of the motion segments does not adequately describe the in vivo behavior. The reason for this is not clear. All the elastic properties in this model were taken from published reports of adult material without scoliosis. It may be that the passive stiffness of the spinal muscles is important in the sagittal plane and muscles were omitted from the model. Alternatively, it may be that postoperative time-dependent deformations occurred in the discs, and these were better represented by an elastic beam element placed posterior to the disc.

The reduction in spinal curvature in the sagittal plane has been reported as the "flat back" complication of the Harrington procedure[2,20,35] and curved rods have been recommended for preventing it.[6] The forces acting on the spine must be equal and opposite ones acting along a single line joining the saddles of the instrumentation hooks, however. Therefore, a curved rod would only have an effect if it directly contacts intermediate vertebrae. This was checked for by calculating the distance from each vertebra center to the rod, and no such contacts were found.

Both measured and simulated changes in vertebral and ribcage rotations in the transverse plane were small and within measurement accuracy. Several other studies have reported minimal changes in vertebral rotation[1,5,8,38] and back surface shape[16,38] after Harrington surgery. Intraoperative rib hump measurements[10] showed small reductions, but only after the application of a convex side compression rod.

Changes in regions remote from the instrumentation were dependent on the boundary conditions. Based on the models' predictions of the correction of "secondary" curves, these worked well. The boundary conditions prevented changes in spinal "balance" (decompensation) despite reported small improvements with the Harrington procedure.[4,5] In the patients studied here, changes in spinal "balance" were within measurement precision.

The studies of sensitivity of the model to the removal of the ribcage showed that model response was predominantly determined by the spinal flexibility. This suggests that operations to release the ribcage (costoplasty) should not be expected to change the degree of spinal correction. Other instrumentation designs intended to produce greater axial rotation correction might be more sensitive to ribcage stiffness.

The model validation was complicated because the measured geometric changes as documented by stereo roentgenograms were taken several weeks apart with the patients standing and often wearing a brace, whereas the model represented surgery done with the patients anesthetized and supported on the operating table. We assumed that postoperative shape changes were negligible. Another possible limitation was that we did not measure hook distraction directly, but instead calculated it from preoperative and postoperative stereo roentgenographic measurements. The good agreement between model and radiographic measurements in the frontal plane, however, suggests that these calculations were accurate.

This work has shown the importance of using individualized three-dimensional geometry in the simulation of surgical correction of scoliosis. Further improvements in the model must depend on a better understanding of the biomechanical or anatomic reasons for the improvements produced by the rigid offsets in the motion segment beams.

■ Acknowledgment

Assistance with formulation of the models was given by Dr. Jeffrey P. Laible.

References

1. Aaro S, Dahlborn M. The effect of Harrington instrumentation on the longitudinal axis rotation of the apical vertebra and on the spinal and rib cage deformity in idiopathic scoliosis studied by computer tomography. Spine 1982;7:456–62.

2. Aaro S, Öhlen G. The effect of Harrington instrumentation on the sagittal configuration and mobility of the spine in scoliosis. Spine 1983;8:570–4.

3. Ashman RB, Birch JG, Bone LB, Corin JD, Herring JA, Johnston CE, Ritterbush JF, Roach JW. Mechanical testing of spinal instrumentation. Clin Orthop 1988;227:113–25.

4. Bassett GS, Hensinger BS, Keiper MD. Effect of posterior spinal fusion on spinal balance in idiopathic scoliosis. J Pediatr Orthop 1989;9:672–4.

5. Benson DR, DeWald RL, Schultz AB. Harrington rod detraction instrumentation. Its effect on vertebral rotation and thoracic compensation. Clin Orthop 1977;125:40–4.

6. Casey MP, Asher MA, Jacobs RR, Orrick JM. The effect of Harrington rod contouring on lumbar lordosis. Spine 1987; 12:750–3.

7. Dansereau J, Stokes IAF: Measurements of the three-dimensional shape of the rib cage. J Biomech 1988;21: 893–901.

8. Dowell JK, Powell JM, Webb PJ, Morley TR. Factors influencing the result of posterior spinal fusion in the treatment of adolescent idiopathic scoliosis. Spine 1990;15:803–8.

9. Fitch RD, Turi M, Bowman BE Hardaker WT. Comparison of Cotrel-Dubousset and Harrington rod instrumentations in idiopathic scoliosis. J Pediatr Orthop 1990;10:44–7.

10. Gaines RW, McKinley CM, Leatherman KD. Effect of the Harrington compression system on the correction of the rib

hump in spinal instrumentation for idiopathic scoliosis. Spine 1981;6:489–93.
11. Gardner-Morse MG, Laible JP, Stokes IAF. Incorporation of spinal flexibility measurements into finite element analysis. J Biomech Eng 1990;112:481–3.
12. Ghista DN, Viviani GR, Subbaraj K, Lozada PJ, Srinivasan TM, Barnes G. Biomechanical basis of optimal scoliosis surgical correction. J Biomech 1988;21:77–88.
13. Haderspeck K, Schultz A. Progression of idiopathic scoliosis. An analysis of muscle actions and body weight influences. Spine 1981;6:447–55.
14. Jayaraman G, Zbib HM, Jacobs RR. Biomechanical analyses of surgical correction techniques in idiopathic scoliosis: Significance of biplanar characteristics of scoliotic spines. J Biomech 1989;22:427–38.
15. Jefferson RJ, Weisz I, Turner-Smith AR, Harris JD, Houghton GR. Scoliosis surgery and its effect on back shape. J Bone Joint Surg [Br] 1988;70:261–6.
16. Johnston II CE, Ashman RB, Sherman MC, Eberle CF, Herndon WA, Sullivan JA, King AGS, Burke SW. Mechanical consequences of rod contouring and residual scoliosis in sublaminar segmental instrumentation. J Orthop Res 1987;5:206–16.
17. King HA, Moe JH, Bradford DS, Winter RB. The selection of fusion levels in thoracic idiopathic scoliosis. J Bone Joint Surg [Am] 1983;65:1302–13.
18. Luk KDK, Leong JCY, Reyes L, Hsu LCS. The comparative results of treatment in idiopathic thoracolumbar and lumbar scoliosis using the Harrington, Dwyer, and Zielke instrumentations. Spine 1989;14:275–80.
19. Meade KP, Bunch WH, Vanderby R Jr, Patwardhan AG, Knight GW. Progression of unsupported curves in adolescent idiopathic scoliosis. Spine 1987;12:520–6.
20. Mielke CH, Lonstein JE, Denis F, Vandenbrink K, Winter RB. Surgical treatment of adolescent idiopathic scoliosis. A comparative analysis. J Bone Joint Surg [Am] 1989;71:1170–77.
21. Nasca RJ, Lemons JE, Walker J, Batson S. Multiaxis cyclic biomechanical testing of Harrington, Luque, and Drummond implants. Spine 1990;15:15–20.
22. Panjabi MM. Biomechanical evaluation of spinal fixation devices: I. Conceptual framework. Spine 1988;13:1129–34.
23. Panjabi MM, Brand RA, White AA. Three dimensional flexibility and stiffness properties of the human thoracic spine. J Biomech 1976;9:185–92.
24. Patwardhan AG, Bunch WH, Meade KP, Vanderby R, Knight GW. A biomechanical analog of curve progression and orthotic stabilization in idiopathic scoliosis. J Biomech 1986;19:103–17.
25. Schultz A, Haderspeck K, Takashima S. Correction of scoliosis by muscle stimulation. Biomechanical analyses. Spine 1981;6:468–76.
26. Schultz AB, Hirsch C. Mechanical analysis of Harrington rod correction of scoliosis. J Bone Joint Surg [Am] 1973;55:983–92.
27. Schultz AB, Hirsch C. Mechanical analysis of techniques for improved correction of idiopathic scoliosis. Clin Orthop 1974;100:66–73.
28. Stokes IAF. The axial rotation component of scoliosis. J Orthop Res 1989;7:702–8.
29. Stokes IAF. Report on an error in the published description of a method of measuring axial rotation of vertebrae, reported by Stokes et al. Spine 1991;16:599–600.
30. Stokes IAF, Bigalow LC, Moreland MS. Measurement of axial rotation of vertebrae in scoliosis. Spine 1986;11:213–8.
31. Stokes IAF, Bigalow LC, Moreland MS. Three-dimensional spinal curvature in adolescent idiopathic scoliosis. J Orthop Res 1987;5:102–13.
32. Stokes IAF, Laible JP. Three-dimensional osseo-ligamentous model of the thorax representing initiation of scoliosis by asymmetric growth. J Biomech 1990;23:589–95.
33. Stokes IAF, Gardner-Morse M, Laible JP. Individualized computer models of surgical correction of spinal deformity. Proceedings of the 37th Orthopaedic Research Society, Anaheim, CA, March 1991. Orthop Trans 1991;15:379.
34. Subbaraj K, Ghista DN, Viviani GR. Presurgical finite element simulation of scoliosis correction. J Biomed Eng 1989;11:9–18.
35. Swank SM, Mauri TM, Brown JC. The lumbar lordosis below Harrington instrumentation for scoliosis. Spine 1990;15:181–6.
36. Thometz JG, Emans JB. A comparison between spinous process and sublaminar wiring combined with Harrington distraction instrumentation in the management of adolescent idiopathic scoliosis. J Pediatr Orthop 1988;8:129–32.
37. Vanderby R Jr, Daniele M, Patwardhan A, Bunch W. A method for the identification of in-vivo segmental stiffness properties of the spine. J Biomech Eng 1986;108:312–6.
38. Weatherley CR, Draycott V, O'Brien JF, Benson DR, Gopalakrishnan KC, Evans JH, O'Brien JP. The rib deformity in adolescent idiopathic scoliosis. A prospective study to evaluate changes after Harrington distraction and posterior fusion. J Bone Joint Surg [Br] 1987;69:179–82.
39. Weaver W Jr and Gere JM. Matrix Analysis of Framed Structures. Second edition, New York, Van Nostrand Reinhold Company Inc., 1980, pp 383–5 and 413–7.

Address reprint requests to

Ian A. F. Stokes
Department of Orthopaedics and Rehabilitation
University of Vermont
Burlington, VT 05405-0084